Carbon from Recycled Materials for Solar Thermal Evaporation and Oil Absorption

ABSTRACT

This study investigated the carbonization of recycled materials for solar thermal evaporation and oil absorption. Cotton fabric, cardboard, and wood were carbonized and treated with acidic substances (lemon juice, sulfuric acid, hydrochloric acid) to modify the carbon surface. The effectiveness of the recycled carbon in solar thermal evaporation and oil adsorption was analyzed. Results showed that untreated recycled carbon performed better in solar thermal evaporation due to a larger solar interface area, while acid-treated carbon was less effective. Quantitative thermal analysis revealed significant weight loss in wood between 285-350°C, with an exothermic peak at 345°C. Wood-derived carbon was 30% more efficient in solar water desalination and sewage purification compared to commercial activated carbon. For oil absorption, lemon juice-treated carbon outperformed others by 40%, except for commercial activated carbon, which was 1.5 times more effective due to its high porosity.

Keywords: carbonization; recycled materials; un-treated carbon; acid-treated carbon, activated carbon; solar thermal evaporation; oil absorption.

1. INTRODUCTION

The 21st century has brought about incredible technological innovations that have changed how people live, communicate, and think. Life-saving advances in medicine, the power of artificial intelligence, the ever-continuing pursuit of the cosmos, and the connective force of social media—all these revolutionary changes encourage much-craved economic success and social growth. But amid these breakthroughs, water shortage, global warming, waste management problems, and many other challenges have emerged. At this time, it is crucial to consider the importance of sustainability and to mitigate the damages incurred along humanity's enduring history. On the issue of water shortage, some currently deployed strategies include water recycling, rainwater collection, and desalination. At the forefront of desalination is reverse osmosis (RO) [1,2], which requires large amounts of electricity to pump water through porous membranes to filter out impurities. RO allows for highly effective water purification and suits a wide range of applications, but depending on the region where these systems are installed, the costs of operation can only be justified with the use of fossil fuels [3]. Moreover, the highly concentrated brine, which remains after the desalination of salt water and purification of other water sources, can inflict harm to the local marine ecosystem and plants when discharged into the ocean [4].

To tackle these issues, solar thermal evaporators made from carbonized recycled materials have been considered [5,6]. Such evaporators are cost-effective and environmentally benign. They may offer a solution to desalinating salt water without the need to pursue complex materials or processes. Sunlight provides an essential source of unlimited renewable energy for a variety of applications, including electricity generation [7-13], heating [14-20], and

emerging technologies such as solar sail propulsion [21-24]. As countries around the world struggle to obtain newer and more expensive technologies, the universal accessibility of the sun's energy assumes a key role in bridging this gap. Additionally, carbonized materials become especially appealing due to their natural abundance relying solely on the presence of cellulose within the material. Plant and paper products like cardboard, paper, and cotton clothing, contain ample amounts of cellulose which makes them ideal candidates for producing carbon materials. In 2023, Americans used over 85 million tons of paper. Approximately 1 billion trees are needed for such an amount of paper. In Canada, about 6 million tons of paper and paperboard are used annually. Only 1/4 of Canada's wastepaper and paperboard is recycled. That is why the idea of repurposing waste materials has become more and more attractive. Another application of carbon from recycled materials is for cleaning spilled oil. As is known, oil spilling causes the leakage of liquid petroleum hydrocarbons into the environment, which damages the ecosystem. The marine species are especially vulnerable to spilled oil. Marine birds, mammals, fish, and shellfish could be killed by the release of oils. Malhas and Amadi (2023) [25] reported their research work on preparing carbon from the avocado peel as a bio-absorbent for oil removal from polluted seawater. The results were obtained from the absorption tests on different types of oil including crude oil, diesel, kerosene, and gasoline in seawater. It was found that the avocado carbon displayed excellent adsorption properties.

Besides avocado peel, other materials are recycled for reclaiming carbon. Chen et al. [26] made the delignified wood porous carbon (DWC) by the high-temperature carbonization method. The lignin in the wood was removed by chemical treatment using a mixed solution containing 0.4 M Na_2SO_3 and 2.5 M NaOH. The processed wood was washed in hot water. Then it was submerged in a 2.5 M H_2O_2 solution to boil for 4 h. The dignified wood (DW) aerogels were obtained by freeze-drying. After being pre-treated at 200 °C for 2 h, the specimens were carbonized in a nitrogen flow at high temperatures of 400, 600, 800, and 1000 °C, respectively. Yang et al. [27] introduced a molten salt approach for preparing porous carbon in air. Wood sawdust as the carbon source was treated in the KCl and KOH-containing molten salt. KCl and KOH acted as the structure-guiding agents to adjust the microstructure of porous carbon, which allowed the porous carbon to have improved electrochemical performance.

Green processing of plant biomass into mesoporous carbon was demonstrated by Chen et al. [28]. Four different plant biomass including bamboo, cotton, softwood, and hardwood were taken as the carbon precursors. Porous carbon was generated via the chemical-free approach. The carbon showed a large surface area and unique mesoporous structure, which was used as the support material for catalysis. Treated by heat and water the pore structure of wood can be modified as illustrated by Tsyganova et al. [29]. The effect of the heat treatment and subsequent treatment with water on the pore structure formation in a solid product made of birch sawdust with the addition of phosphoric acid was studied. Natural vessels in wood can provide large space initially for nutrients and water transport during the growth of the tree [30]. The space can also serve as a venue for rapid mass transport of active materials. Luo et al. [31] showed how to construct hierarchical pores while retaining the natural vessels in wood. To maximize the utilization of lignocellulose and avoid complicated extraction, wood with a porous structure and good mechanical strength was used as the carbon precursor. Chemical activation (e.g., by KOH or K_2CO_3) was not used because it destroys the natural structure of wood. Instead, the Lewis reagents such as copper chloride, zinc chloride, and aluminum chloride were used as the activating substances and protection materials. The lignocellulose-rich poplar wood was used as the carbon source material. The poplar wood was soaked in one of the Lewis agents at 20%. Then, carbonization was conducted at 900 °C in nitrogen for 2 h.

Cotton contains more than 90% cellulose. It is a promising raw material for the fabrication of carbon-based materials by direct carbonization or activation process. Hao et al. [32] made porous carbon from natural cotton via a simple one-step eco-friendly method. The cotton was dried at 200℃ and carbonized at 550, 650, and 750℃ to generate carbon with a specific surface area of 480 m^2/g. Waste cotton was also considered for generating porous carbon [33,34]. Thach et al. [33] prepared the ultrahigh porosity activated carbon (AC) from the H_3PO_4-impregnated waste cotton precursor through carbonization in Ar. Then, the physical activation in variable CO_2 flow rate with ultrahigh heating rate. Was performed. It was found that CO_2 played an important role in activating cotton carbon for the formation of the highly porous structure. The specific surface area and micropore volume reached 4,800.7 m^2/g and 2,499 cm^3/g, respectively. Recycling the waste cotton from the textile industry for carbon production was shown and the obtained porous carbon was used to build interfacial solar evaporators for water purification [34].

Wastepaper and waste cardboard would cause environmental problems if not appropriately disposed of. Recycling wastepaper and cardboard is of great interest to green economics and environmental sustainability [35]. Shimada et al. [36] prepared activated carbon from waste newsprint paper and a specific surface area of 1,000 m^2/g for the carbon was achieved. The absorption property of the carbon from the waste newsprint paper was comparable to that of the commercially available activated carbon. In literature [37], activated carbon was also made from wastepaper. Specifically, kraft bags, with very low ash content, were recycled to generate activated carbon. Small pellets of the wastepaper were continuously extruded from a kneader. Carbonizing the pellets in nitrogen was performed. Following that, the activation was done in carbon dioxide. The Brunauer-Emmett-Teller (BET) specific surface area of the activated carbon prepared from the waste kraft bags reached 1,285 m^2/g, which is higher than that of commercial activated carbons. The activated carbon prepared from wastepaper has a well-developed porous structure, particularly in the mesopore range [37].

Recycled carbon fibers have found many applications. Crespo-Lopez et al. [38] showed that the carbon fiber from wind turbine blades can be added to bricks for construction. The fiber made the bricks more durable against salt crystallization. Recycled carbon from bamboo was reported for dye absorption. [39]. Murugesan et al. [40] recycled waste sugarcane bagasse to make porous conductive carbon-containing macropores for capacitive energy storage application. In recent study by Gautam et al. [41], pyrolysis of biomass to generate activated hydrochars as sustainable materials for removing pharmaceutical contaminants from water was discussed. The recycled carbon materials showed peculiar pore structures and large surface areas, which allowed them to demonstrate high adsorption capabilities.

In this work, several carbonized materials were produced from recycled sources by controlling the carbonization conditions. Various acids were used to treat the recycled carbon with the intent of introducing as many oxygen-containing functional groups and structural defects in the carbon as possible. It was revealed that the acidic treatment can modify the carbon surface by introducing oxygen-containing functional groups so that active sites for holding other materials can be generated [42]. The acidic treatment could enhance the wetting between polar solvents and the recycled carbon. It is hypothesized that the solar thermal evaporation and oil absorption behavior of recycled carbon could be changed due to the introduction of oxygen-rich functional groups. The generated carbon products will be tested in view of their effectiveness in enhancing solar thermal evaporation. The oil absorption behavior of these recycled carbon materials will be evaluated as well. Furthermore, the feasibility of making useful carbon materials from traditional recycling plants will be discussed.

The novelty of the work lies in the integration of both energy sustainability and environmental sustainability. An easily implemented, low-cost, and direct carbonization of recycling materials

to make multifunctional products such as for seawater desalination, sewage water purification and oil adsorption/absorption was demonstrated. The reclaimed carbon from recycled wood, paper, and cotton was surface treated with very low concentrations of chemicals or acid from a sustainable source (lemon). Therefore, the research provides environment-friendly manufacturing processes for carbon production. The thermal gravimetric analysis data allow the start of intensive heat generating from wood to be identified. The work increases our understanding of the temperature dependent decomposition of recycled materials especially wood. Disposing of recycled wood is meaningful in view of wildfire reduction and prevention.

2. MATERIAL AND METHODS

2.1 Carbonization of Wood, Cardboard Paper and Cotton

The recycled wood (Douglas fir), cardboard paper (from packing boxes) and cotton were collected from Orange County, California, USA. The commercial activated carbon was made by Aqua-Tech and purchased from Walmart Supercenter. Two different methods of carbonization were used in this study. In the first method, the top of the carbonization steel chamber was wrapped with aluminum foil. The chamber was placed inside a chimney starter, with charcoal underneath and surrounding the carbonization container as shown in Figure 1(a). In the second method, a butane tank was connected to a burner to heat the carbonization chamber made of a paint bucket as revealed in Figure 1(b). Most of the carbon was made using the chimney starter, shown in Figure 1(a), with heat surrounding the storage vessels. With this iteration of the method, however, the way the cans were originally opened allowed for more airflow, resulting in the materials igniting and whitening afterward. Aluminum foil was subsequently adopted as an additional measure to preserve the samples during the carbonization process. Carbonization took roughly 30 minutes, with temperatures maintained at above 350°C for each container of respective materials. It was noted that paper and cardboard were quickly carbonized, followed by cotton fabric, and then wood.

(a)  (b) 

Figure 1. Photographs showing the carbonization setup: (a) chimney starter configuration, (b) gas burner configuration.

For the carbonization trial involving the gas burner and bucket, shown in Figure 1(b), heat was focused solely on the bottom and temperature dropped off considerably along the height. Consequently, materials required reorienting within the vessel to reach the necessary carbonization temperature. Due to the volume of the paint bucket, the smaller butane burner was unable to distribute heat as thoroughly as the charcoal did for the aluminum-covered steel cans.

In the carbonization experiment, when the vessels no longer emitted flammable smoke, the charcoal should be ready, and the chamber was ready to be cooled down. With this standard in place, the time between making charcoal varied greatly between 15 - 30 minutes for the chimney starter and 75 minutes for the gas burner. The temperature of the reaction chamber generated by the butane burner was about 530°C. Although the temperature of the chimney starter hovered between 230°C - 330°C, the actual temperature inside the chamber should be much higher. It was estimated above 550°C, but lower than the melting point of aluminum foil which is 660°C. All the materials made from the two methods were stored separately. The carbon samples were then ground up using a pestle and mortar and stored in airtight containers.

2.2 Acid Treatment on the Recycled Carbon

To examine the acid treatment effect, nine different samples were tested. Each sample contains 0.5 g of carbonized material submerged in solutions of 2.5 mL of sulfuric acid, hydrochloric acid, and lemon juice, mixed with 2.5 mL of water. Citric acid is a concentrated compound from lemon. Lemon juice contains citric acid, water, vitamin C, and other molecules. Lemon juice was selected based on the availability of natural resources. Using lemon juice that has been squeezed is a more sustainable practice than using concentrated or pure citric acid. Using concentrated citric acid needlessly introduces a more complex step in the acidification process, subsequently increasing the cost. It should be noted that the HCl solution is made of 20 mL 36 wt.% concentrated HCl mixed with 40 mL water, while the sulfuric acid solution has a concentration of 0.12 N. As noted throughout the 72-hour acidification period, the lemon juice took the longest amount of time to activate the charcoal. This observation was made from comparisons with the other acid samples, which in turn was noted by the carbon samples sinking to the bottom of the tubes.

After the 72 hours, the samples were poured from the tubes into coffee filters with a pore size of 20 microns. They were then washed thoroughly with deionized water 3-4 times and then moved into an oven at 115°C for 2 hours to remove excess moisture and activate the surface.

2.3 Solar Thermal Evaporation and Sewage Wastewater Purification

The solar thermal evaporation tests were performed in Orange County, Southern California, USA with abundant sunlight. As shown in Figure 2, the carbon samples were added to a beaker and/or sewage water to form test units. At the same ambient temperature and with equal exposure to sunlight, the weight loss of each unit was recorded at various periods of time. The total time for each sample to evaporate the seawater and sewage water was also recorded.

Figure 2. Test setup for solar thermal evaporation experiment.

2.4 Oil Absorption Test

Oil adsorption testing was done using two different oils: virgin olive oil and used motor oil. 5 mL of each oil was mixed with 5 mL of water to form an immiscible suspension. Then, 5g of each acidic treated carbon was added into the test tubes. The efficacy of each acid-treated carbon was examined and then compared with that of a commercially available activated charcoal. Oil and water were added to a test tube filled with each adsorbate and then stirred until completely saturated. To understand the nature of the water-oil mixture and establish a baseline for observation, separate tubes were prepared without any acid-treated carbon (AC).

2.5 Scanning Electron Microscopic Observation

A typical sample, for example, the wood before carbonization was coated with platinum for 60 s using the Agar Sputter Coater at 40 mA under 0.05 mbar. Morphology observation on this specimen was performed using the JEOL JSM-6360 scanning electron microscope with a Thermo Scientific EDX detector to show the initial cellular and porous features in the recycled wood.

2.6 Quantitative Thermal Analysis

The quantitative thermal analysis of wood was performed in this study. Thermogravimetric Analysis (TGA) was carried out to determine the decomposition/mass loss over a temperature range from 23 °C to 900 °C. The Differential Thermogravimetry (DTG) data were obtained to determine the exothermic event temperature associated with the oxidative decomposition of the wood sample in air. A TGA50 Shimadzu Thermogravimetric Analyzer purchased from

Shimadzu Scientific Instruments, Inc., Columbia, MD, USA, was used for the TGA experiment. The sample with a weight of 8.337826 mg was used to generate the time dependent weight data when the temperature was raised at a rate of 10 °C /min.

2.7 BET Surface Area and Porosity Measurement

The BET surface area and porosity analysis of the porous carbon derived from typical recycled materials, e.g., Douglas fir wood, were performed through the BET method using a Micromeritics 3-Flex Surface Characterization System, from Micromeritics, Norcross, Georgia, U.S.A.

3. RESULTS AND DISCUSSION

3.1 Carbonization

During the carbonization process, it was noticed that some of the materials, namely cotton and cardboard paper, carbonized more quickly and it was possible to exchange them for new materials. On a closer level, it was also noticed that, while some materials were carbonized, others had been somewhat protected from the heat, possibly due to insulation from other materials. For simpler heating systems or systems with uneven heating, a suggestion may be to occasionally agitate the materials for more even carbonization.

Close monitoring and understanding of the time and heat thresholds required to carbonize a material would greatly increase production efficiency. During the acidification process, consistent hydrophobicity, especially for cotton, was observed for many of the samples, and occasional stirring was required to ensure complete amalgamation. The acidic treatment of carbon could introduce many oxygen-containing functional groups and structural defects in the carbon [42], which may assist the wettability of water on the recycled carbon. The solar thermal evaporation and oil absorption behavior of recycled carbon could be changed due to the introduction of oxygen-rich functional groups.

Due to the small size of the carbonized particles, it may have proven beneficial to separate the larger particles using a sifter before beginning the washing process, where the largest amount of material was lost. Additionally, a filter with a smaller pore size combined with a vacuum filter system would have provided a more robust method for increasing yield. Because the recycled materials can all convert to carbon, another study where these materials are carbonized, powdered, and acidified together may be worth conducting.

3.2 Microstructure

The photographs of various samples are shown in Figure 3. Nine representative samples with the information are presented. From left to right, samples A, B, and C are carbonized samples from recycled cardboard paper in sulfuric acid, lemon juice, and hydrochloric acid; samples D, E, and F are carbonized wood samples in sulfuric acid, lemon juice, and hydrochloric acid; samples G, H, and I are carbonized cotton samples in sulfuric acid, lemon juice, and hydrochloric acid.

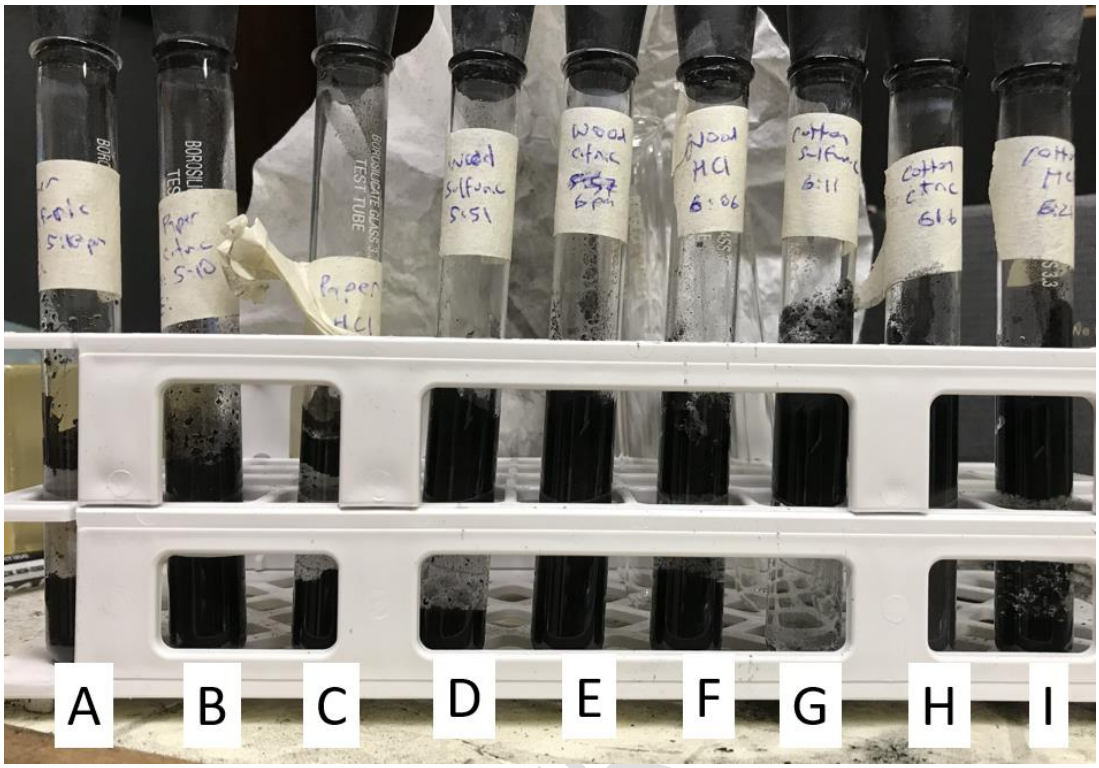

Figure 3. Photographs showing nine carbonized samples in acids.

The initial structure of the wood was examined by scanning electron microscopy (SEM) at an acceleration voltage of 20 kV and the images captured at a working distance of 15 mm are shown in Figure 4. Before the SEM imaging, the sample was sputter-coated with Pt to reduce the discharge of electrons. The transverse cross-section view of the wood in Figure 4(a) shows a cellular structure with pores and cracks separating the year-ring of the original tree. In Figure 4(b), the longitudinal cross-section of the wood reveals parallel grooves along the axial or the tree-growing direction. Some fibers can also be found in the image. In either direction of view, the wood is characterized by pore-rich morphology. Such a unique structure is the origin of porous carbon formation under high-temperature pyrolysis.

(a) 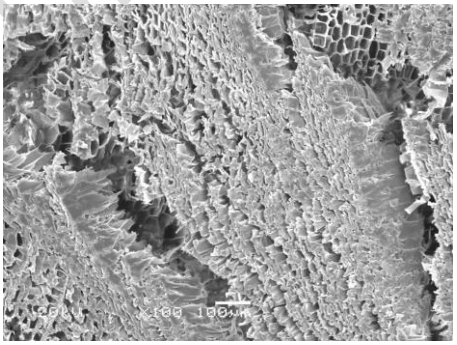

(b) 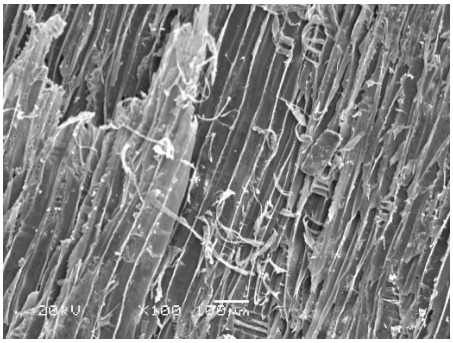

(c) 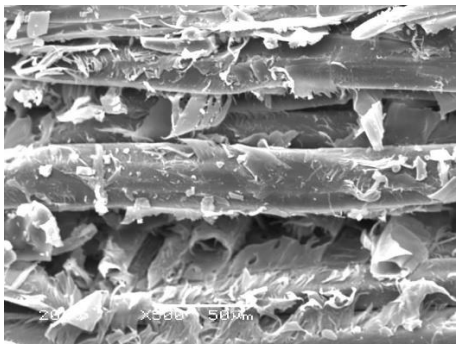

(d) 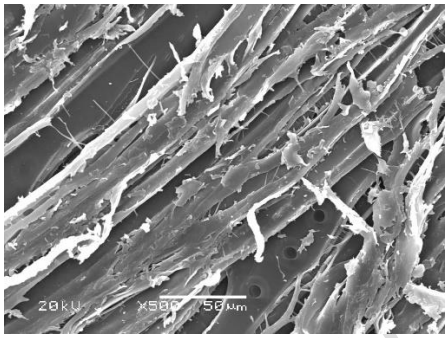

Figure 4. Scanning electron microscopic images of wood before and after carbonization: (a) transverse cross-section view of wood before carbonization, (b) longitudinal cross-section view of wood before carbonization, (c) higher magnification showing the layered structure of wood before carbonization, (d) the shrinkages and cracking of the ligaments, pore expansion and fibrillation of wood after carbonization.

3.3 Thermogravimetric and Differential Thermogravimetric Analysis Results

Quantitative thermal analysis of wood was specifically performed in this study. The thermogravimetric analysis (TGA) was carried out in air. The results will help validate the manufacturing process. The decomposition/mass loss over a temperature range from room temperature (23 °C) to a selected high temperature of 900 °C in air provide the guideline of how to control the burning and muffle the container or chamber holding the specimens to obtain the derived carbon instead of ash. As shown in Figure 5, the weight (*W*) of the wood in air started dropping just above 280 °C. The major loss of its weight loss peak appeared at 340 °C as marked by the vertical blue line. During the manufacturing processes, the temperatures measured were above 530 °C. Since the specimens were well muffled by the metal foil, this confirmed the carbon formation from the recycled wood. If the wood should burn in air, it would convert its original weight to about 3.5% of ash. In Figure 5, the differential thermogravimetry (DTG) data were also presented which were obtained by taking the derivative of weight loss with respective to the time, *t*. The DTG results allowed us to determine either the endo- or exothermic event temperatures associated with the oxidative decomposition of the wood sample in air. Obviously, the peak located around the temperature of 340 °C indicated that the wood would generate intensive heat if it were exposure to air.

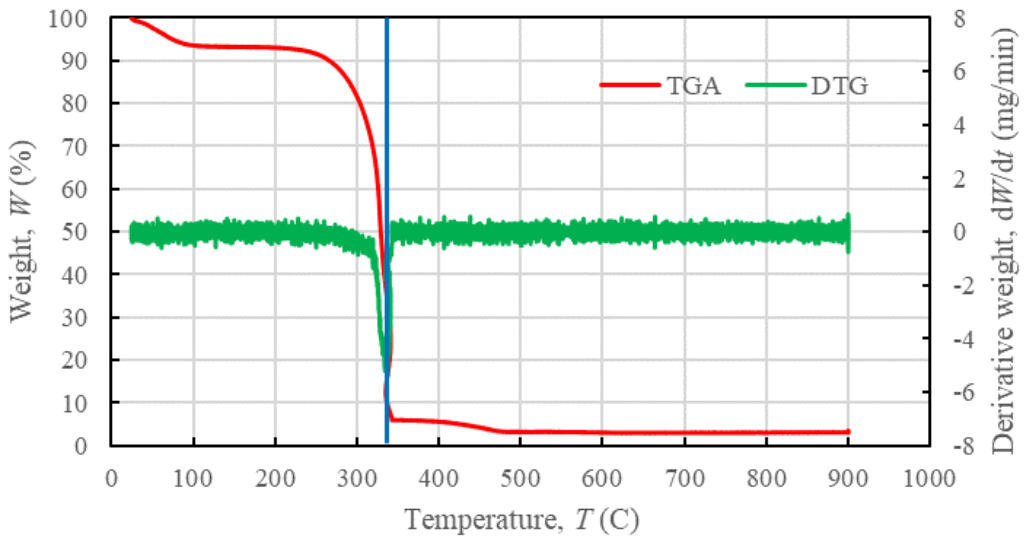

Figure 5. **TGA and DTG of wood in the temperature range from 23 to 900 °C**

3.4 Solar Thermal Evaporation Behavior

The first and the second columns in Table 1 show the combinations of adsorbates and solutions used in the evaporation testing. To set the test conditions close to the real-world application scenarios, all the tests were done with 5 g of the carbon materials mixed with 100 mL of either seawater or sewage into 12 separate beakers. The seawater was fetched from the Pacific coast of Orange County, California, USA. Sewage was obtained from the Midway City Sanitary District in Westminster, California, USA. Due to a limited number of alternative acids and beakers, the activated samples of paper, cotton, and wood were acidified using only lemon juice. Additionally, two of the beakers were prepared with 100 mL of sewage and seawater as references.

Table 1. Materials and fluids used for solar thermal evaporation tests and the results.

Sample Number	Material Added	Type of Liquid	Evaporation time (h)
1	Paper, AC[1]	Seawater	70.15
2	Cotton, AC	Seawater	71.15
3	Wood, AC	Seawater	70.15
4	Wood, UAC[2]	Seawater	49.45
5	Cotton, UAC	Seawater	69.15
6	Paper, UAC	Seawater	54.55

7	None	Sewage	N/A
8	None	Seawater	N/A
9	Commercial CAC[3]	Seawater	71.15
10	Wood, AC	Sewage	59.75
11	Cotton, AC	Sewage	71.15
12	Paper, AC	Sewage	69.15

[1] Acid Treated (AC), [2] Un-Treated (UAC), [3] Commercial Activated Carbon (CAC).

In addition to the acid-treated (AC) samples for testing, un-treated (UAC) charcoal samples also provided some interest due to their similar composition. Visually, the two types of samples are identical, but potentially there would be an increase in surface area from the surface modification effects of the citric acid in lemon juice and the other two inorganic acids. Prior to evaporation testing and exposure to the sun, the samples were observed after mixing. Both AC and UAC samples reacted similarly with seawater. The recycled carbon derived from the wastepaper was slightly hydrophobic. The cotton-derived carbon was extremely hydrophobic. Both the wood-generated carbon and the commercially available activated carbon (CAC) were hydrophilic. All samples reacted with effervescence upon mixing. For sewage, all samples reported much easier-to-reach saturation with little to no effervescence.

After 3 hours, the samples were observed again and it was noted that all the AC and UAC samples, except for the CAC, were still heavily obscured with carbon particles. In the case of the sewage samples, little effervescence was noted, and a green tinge appeared with the blackness of the carbon. A small sedimentary layer had also formed at the top and the bottom of each sample, possibly due to the complete saturation of the carbon material. The commercially available activated carbon (CAC) developed a very thin layer with the majority seeping to the bottom. Similarly, the AC samples with sewage displayed very thin layers. However, the AC and UAC samples mixed with seawater showed more prominent top layers, spanning ~20 mL in volume.

Due to the constrained daylight hours of the fall and winter seasons, the samples were periodically exposed to sunlight on a rooftop, where shade and other obstacles would be minimal. At sunset, the samples were covered and brought into a stable environment for overnight storage. Salinity testing was done using a swing-arm salinity hydrometer.

To evaporate every sample excluding the pure sewage and seawater samples, the total exposure time to sunlight was conducted for each sample. The third column in Table 1 lists the amount of time needed to evaporate 100 mL of seawater and sewage water with the added recycled carbon. The longest time needed is 71.2 h for the cotton-derived carbon specimen and the commercial activated carbon as well.

Figure 6(a) and (b) show the respective charts for the seawater and sewage test cases. Sewage evaporated at a much higher rate than seawater did, and the UAC samples assisted by the largest amount in increasing the evaporation rate. Part of the explanation is due to the higher concentration of salt in seawater and the slightly green color of sewage that promoted higher solar absorption. More importantly, the results demonstrate the positive effect of the

acidic treatment on the recycled carbon. As indicated in [42], the acid treatment of carbon black produces additional oxidized functional groups on the carbon surface and defects in the carbon bonding. This would enhance the seawater wetting on the carbon and allow better mass and energy transport during the solar thermal evaporation. However, the entrances of the carbon pores may be blocked by these surface modifications if too much time for acidic treatment is conducted. Therefore, the time of processing is a parameter that affects the performance of the recycled carbon.

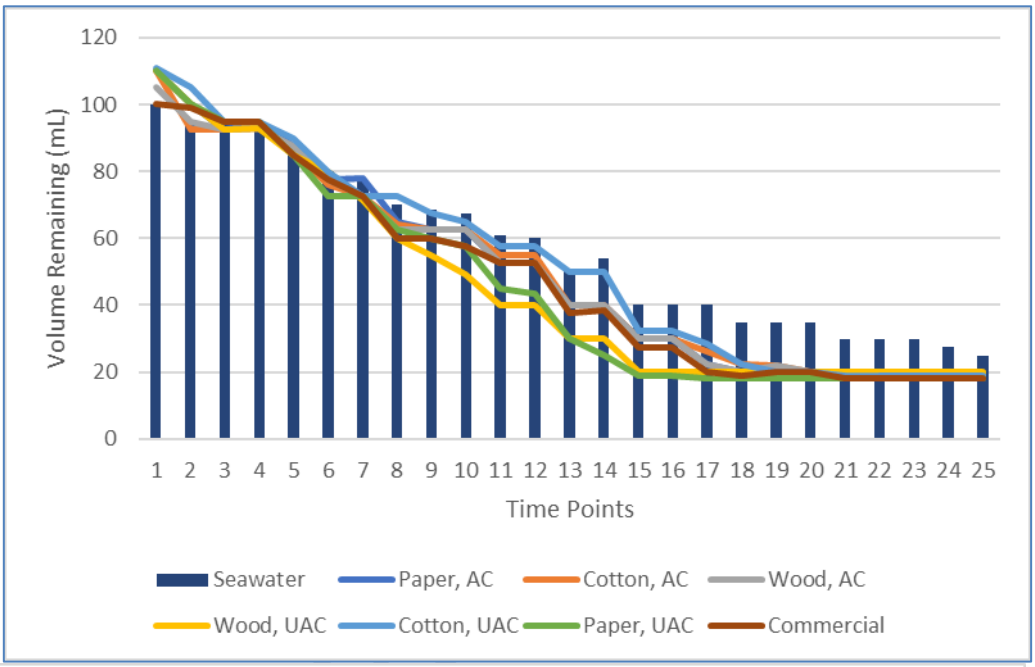

(a)

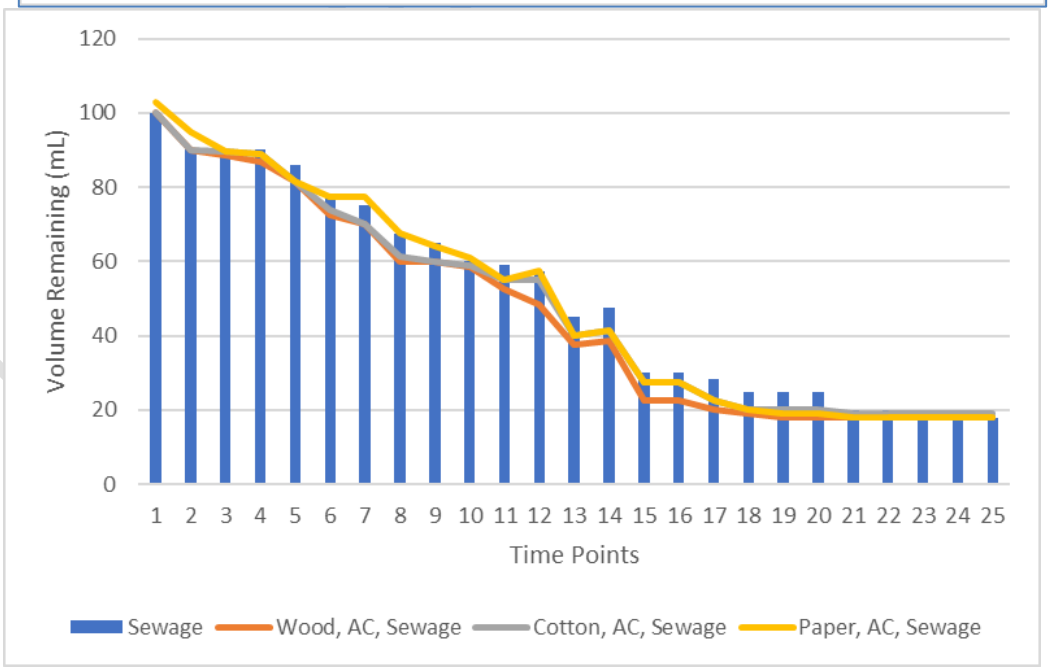

(b)

Figure 6. The solar thermal evaporation test results: (a) acid-treated carbon in seawater, (b) acid-treated carbon in sewage.

In Figure 6(a) and (b), the time points represent times during the day for which evaporation was conducted. Testing was done over 9 days using approximately 9 hours of sunlight with varying irradiation and weather conditions. Points 1-3, 4-6, 7-8, 9-11, 12-13, 14-15, 16-18, 19-21, and 22-25 each represent respective times when the remaining volume was measured. The lines represent the volumes of the AC and UAC samples while the bars represent the volumes of the seawater and sewage controls.

During initial testing, a volume of roughly 20 mL of acid-treated carbon floated on the top, forming a layer, for most of the cases. It is widely known that evaporation occurs at the surface and using this information, the idea of solar interfacial evaporation has grown in recent years [43]. From this principle, it is hypothesized that the most capable samples would feature consistent layers at the water surface. Based on the blackness of UAC and AC carbon samples by nature, the ability to absorb sunlight and increase temperature was expected to also increase evaporation. Due to the denser nature of seawater, the weight of the carbonized materials is largely supported above it by its higher porosity, lower density, and slightly hydrophobic properties. It is due to this nature that stirring of the highly hydrophobic cotton samples was required initially (though stirring was not limited to cotton) to ensure proper absorption of each fluid. It is believed that the evaporation rate has a direct correlation to a material's ability to maintain the solar interface.

Initially, among the AC seawater samples, cases 1, 3, and 9 reported the thinnest top layers, so evaporation was not expected to increase substantially. Case 2 had a thicker layer and was expected to perform on a similar level as the UAC samples. For the sewage samples, all samples had a thin top layer, which contributed to poorer evaporation results. However, as the amount of liquid dropped further, as seen in time points 16 and 17 of Figure 5(a) and (b), the evaporation rate increased. This may be due to the lower layer acting as a heating element or interface.

During and after testing, the salt buildup of the samples was discerned. The largest amount was noticed with the UAC samples in salt water, followed by the AC samples in salt water, and then the sewage samples. Based on the buildup along the beaker walls, the AC had a higher affinity for adsorbing salt, indicating that acidification did have some effect, and it was observed that these effects resembled that of commercial AC.

As a material, cotton appeared to have the lowest evaporation rate among both the UAC and AC samples, placing last for both seawater and sewage cases. Wood performed the highest, with UAC placing first and AC placing third. UAC paper placing 2nd, with a 6-hour gap between it and the AC wood, implies that both material and activation status play a part in improving the evaporation rate. Figure 7 shows that, despite being untreated, cotton may be a much poorer catalyst for evaporation than wood, even for activated wood. UAC tests with sewage, which evaporates more quickly, would cement the hypothesis that activation decreases the evaporation rate.

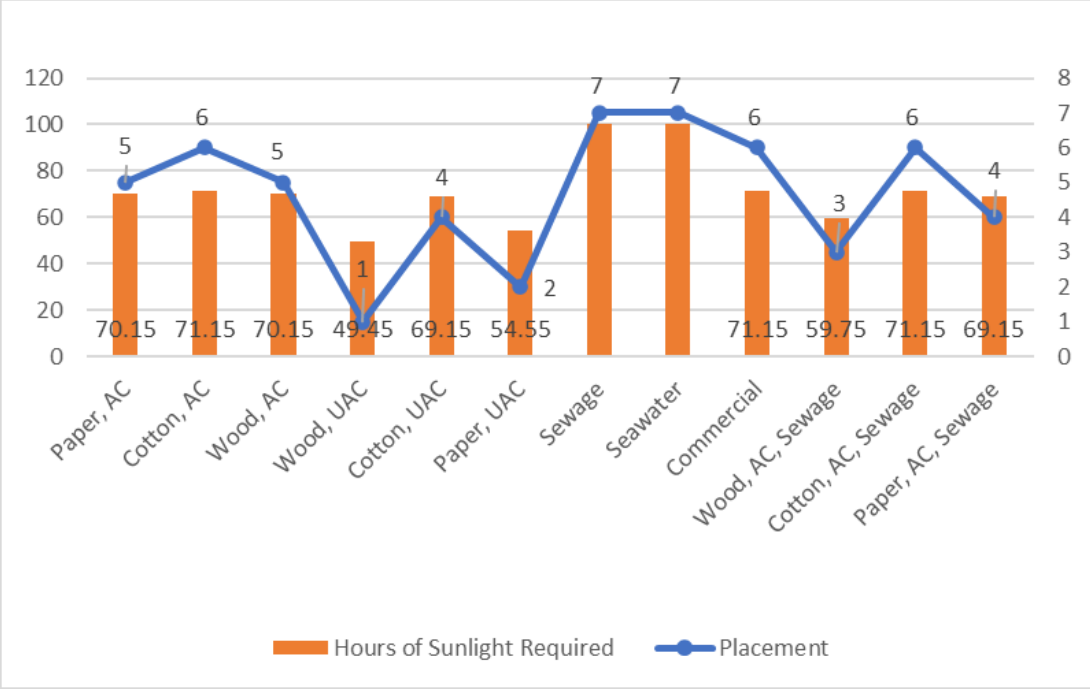

Figure 7. Hours of sunlight are required to evaporate 100 mL of liquid. (Note: The evaporation hours for the control samples of sewage and seawater without any carbon addition were not recorded.)

One point of interest that emerged during this study occurred during the transfer of beakers from the contained space back onto the rooftop. While stored in the dark, all the samples appeared murkier and then cleared up as exposure to the sun increased. This photochemical behavior suggests that other chemical reactions may be occurring between the seawater and the carbon. A study on the photochemical behavior of AC was done where AC had regenerated itself to about 30% of its initial capacity under light [44].

Activated carbon can trigger the photo-oxidations of organic pollutants, even without the presence of conventional semiconductor additives such as TiO_2. This is because the water dissociation can be enhanced at the activated carbon/water interface as shown in [44], i.e.,

$$\boldsymbol{h\nu + H_2O \rightarrow HO\cdot + \cdot H} \quad (1)$$

Presume sewage water and seawater contain hydrocarbon emulsions and are exposed to sunlight. In addition to the water disassociation as described in Eq. (1), the following photochemical reaction happened at the carbon/sewage water or seawater interface.

$$\boldsymbol{h\nu + \{R\}_{m+n} \rightarrow \{R\}_m\cdot + \cdot\{R\}_n} \quad (2)$$

where $\{R\}_{m+n}$, represents a higher molecular weight hydrocarbon organic compound containing $m+n$ carbon atoms. $\{R\}_m\cdot$ and $\{R\}_n\cdot$ are hydrocarbon radicals. They contain m and n carbon atoms, respectively. m and n are integers.

Now, the chain termination of $\{R\}_m\cdot$ and $\{R\}_n\cdot$ by $HO\cdot$ and $H\cdot$ generate various lower molecular weight alcoholic and hydrocarbon compounds. The continued dissolution of the lower molecular weight compounds such as $\{R\}_m$, $\{R\}_n$, $\{R\}_m$OH, $\{R\}_n$OH etc. eventually resulted in the decomposition of the organics in water.

The UAC and AC samples had darkened from the lack of sunlight and began clearing, showing that the above reactions in both Eqns. (1) and (2) occurred in this study. The movement of the

AC implies that the components within the sewage and seawater may be mixing more thoroughly using the sun's energy. This means that a stirring mechanism is potentially already available, allowing the AC sample to adsorb as much as possible over time.

Figure 8 shows the accumulative amount of evaporated water at different times and the evaporation rate of water for the wood derived carbon. The total amount of water is 100 mL held in a 100 mL beaker with a diameter of 40 mm. From Figure 8(a), during the total test period of 49.45 h, the water evaporated within about 31.5 hours. The rest of the 18 to 19 mL water remained because the porous carbon held the absorbed water within the pores at ambient temperatures. Figure 8(b) presents the evaporation rate of water from both sewage water and seawater. The average rate of evaporation from sewage water is about 1.9277 kg/m^2·h within the first 31.5 hours. The average rate of evaporation from seawater is about 1.9194 kg/m^2·h within the first 31.5 hours which is slightly lower than that of the evaporation from sewage water. This is reasonable because seawater has a higher brine concentration. The brine could slightly increase the boiling point of seawater. However, the impurities in sewage also had the boiling point elevating effect. Consequently, there is no significant difference in the evaporation rates of these two waters.

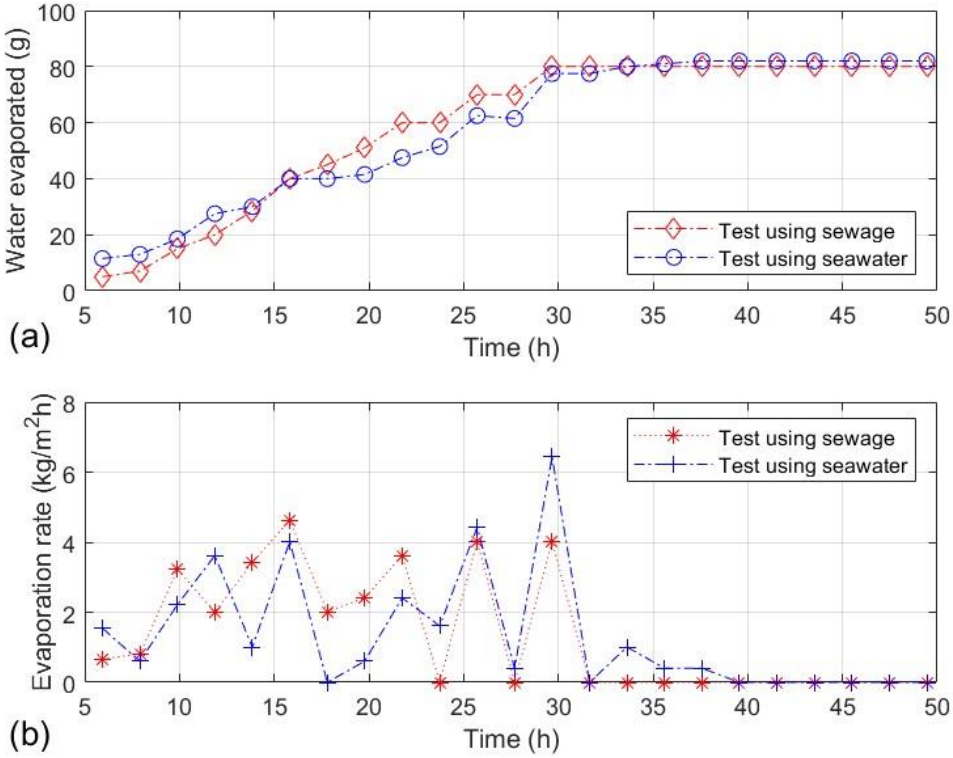

Figure 8 Solar thermal evaporation performance of the wood derived carbon being tested in sewage water and seawater: (a) accumulative water evaporation amount, (b) water evaporation rate.

Given the results of the evaporation study, the extra resources spent to activate the carbonized materials do not seem cost-effective if evaporation is the main objective. Of the UAC materials, wood derived carbon emerged as the most effective at increasing the evaporation rate, though, on a larger scale where the option of recycled materials is not a privilege, it may be

worthwhile to consider mixing materials to retain the best results from each AC or UAC. Further testing would be required to make any conclusive statements. Based on the solar thermal evaporation test results, it can be inferred that AC was more successful in adsorbing salts than UAC was, based on the amount of residue left on the beaker walls. Wood AC carbon was the most efficient at adsorbing the salt throughout the evaporation process. In this study, only 5 g of material was used in each case but varying the amounts of AC/UAC to achieve the most cost-effective solution for an evaporation system may be an idea for another study. Testing with different storage mediums and with different amounts of AC and UAC or fluids would help further define the ideal conditions for these materials in evaporation.

3.5 *Oil Absorption Behavior*

Totally 20 specimens were tested as shown by the test matrix in Table 2. During the olive oil test cases, results were observed in irregular time intervals, e.g., for olive oil, the effects of AC on oil were viewed after 9 hours, 24 hours, and then after 2 weeks. Due to the infrequency and irregularity of the observation periods, there are no confident remarks to be made on the steady-state times for a sample of AC. Additionally, when a sample would appear to reach a steady state, the AC was periodically agitated to facilitate homogenization. No UAC samples were tested with the oil.

Table 2. The oil absorption test matrix shows sample information and types of oil used.

Material & Treatment Solution	Oliver Oil	Motor Oil
Paper, H_2SO_4	A_1	B_1
Paper, LJ[1]	A_2	B_2
Paper, HCl	A_3	B_3
Wood, H_2SO_4	A_4	B_4
Wood, LJ	A_5	B_5
Wood, HCl	A_6	B_6
Cotton, H_2SO_4	A_7	B_7
Cotton, LJ	A_8	B_8
Cotton, HCl	A_9	B_9
Commercial activated carbon	A_{10}	B_{10}

[1] lemon juice.

The binding of oil molecules to the surface of AC is driven by Van der Waals forces, which arise from the fluctuations between electrons within a molecule. Though weak, AC provides a large contact area and porosity driven by the activation process [3]. Figure 9(a) shows control samples used to understand the natural state of these adsorbates without any AC. Because oil and water are two naturally immiscible liquids, the ability of the AC to adsorb the oil was determined by how much of the original color remained compared to the results of the commercial AC.

The relationship between the oil and commercial AC is perceived as cohesive. Upon shaking the tube, the AC particles would disperse, but then gradually collect to reform a similar structure. This behavior was consistent each time the tube was agitated. Figure 8(b) shows the samples after 2 weeks of intermittent agitation.

(a)  (b) 

Figure 9. (a) Control samples of 5 mL of used motor oil and olive oil and (b) AC samples in olive oil after testing for 2 weeks. Case A_{10} can be seen on the far left for the commercially available activated carbon (CAC).

In Figure 9(b), the commercially available activated carbon (CAC) shows that three layers have formed. Because water is denser than oil, it seeps to the bottom, and the cause may be due to the CAC adsorbing components from the water and oil together. When the tube was agitated, it is possible that the CAC bound itself to the oil but was caught between the density of the water. Another test allowing just CAC and oil to mix and reach a steady state, followed by the addition of water, would further narrow the range of hypotheses.

After one week of testing on the paper-derived carbon with acid treatment, roughly half of the AC was successfully adsorbed by the samples in cases A_2, A_1, and A_3. The prominent layers of yellow oil were present at the top, suggesting that the acidification process may have been inadequate for activation, or the carbon derived from paper has a lower affinity for oil adsorption. The bottom layer of AC may be potentially due to an amount of AC that had adsorbed oil but is also creating a seal against the bottom of the test tube itself due to its hydrophobic properties. Because the AC is denser than water, this phenomenon may also be the result of the strong adsorptive abilities of more porous AC or even from the geometry of the tube. As noted from the evaporation study done within this overall project, commercial AC sinks to the bottom of the container naturally, while typical char-material floats and sinks. Between the two, it is possible that the density and the increased porosity invoked by activation are the forces holding down the bottom layer. To understand more precisely when a sample of carbonized material becomes activated, a Brunauer-Emmett-Teller (BET) surface area analysis test would provide the most accurate reading of just how much more the surface area was increased due to acidification. According to Januszewicz et al. [45], the BET surface area for the carbon derived from locally recycled wood in Poland was about 27.3 m^2/g, and the pore volume was about 0.013 cm^3/g. In this work, high BET surface area was found for the carbonized Douglas fir. The measured BET surface area for the Douglas fir-derived carbon in current study reached 228.6406 m^2/g. The pore volume of the Douglas fir wood-derived carbon was found to be about 0.118711 cm^3/g, which is eight times higher than that reported in [45]. The isothermal plot is shown in Figure 10(a) and the pore size distribution plot is shown in Figure 10(b). The nitrogen adsorption average pore size was determined as 2.0768 nm.

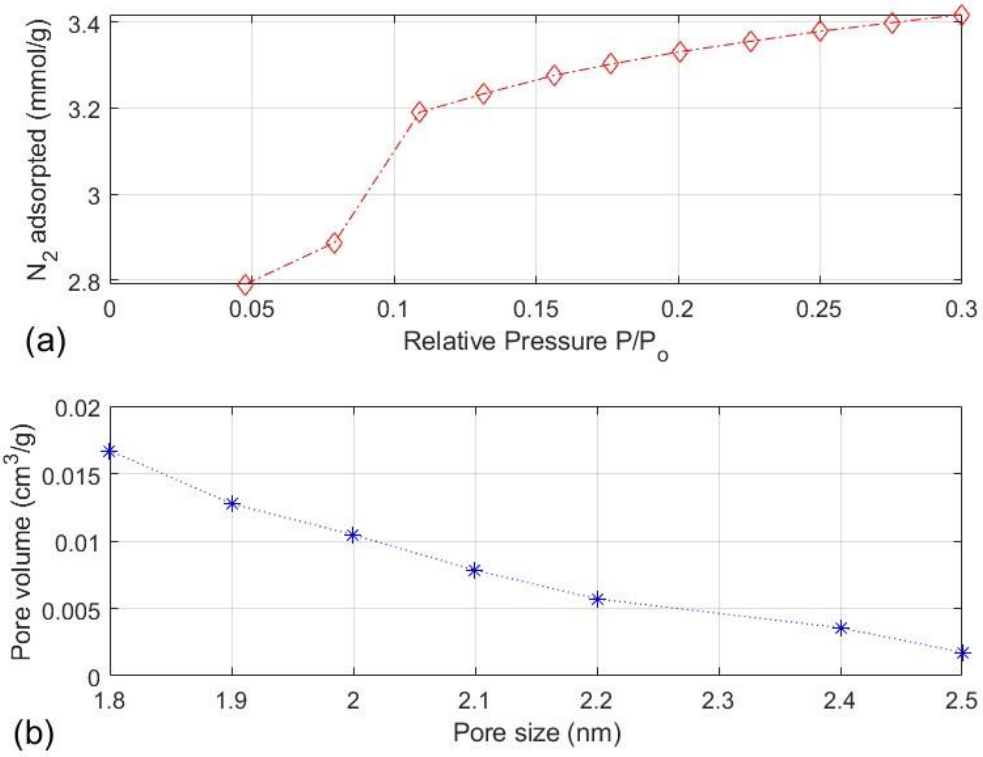

Figure 10. The BET results for the wood derived carbon: (a) isothermal, (b) pore size distribution.

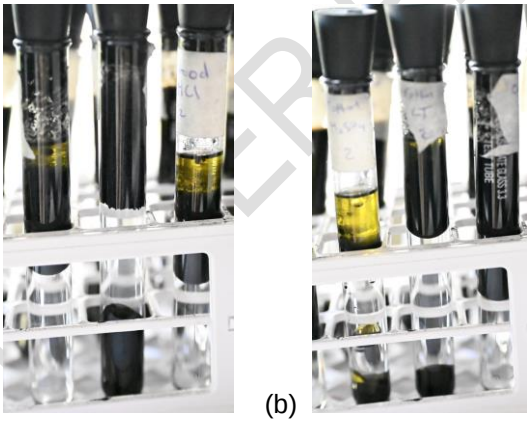

(c)

Figure 11. (a) wood and olive oil results after 1 week for cases A_4, A_5, and A_6 from left to right, (b) cotton and olive oil results after 1 week for cases A_7, A_8, and A_9 from left to right, (c) motor oil cases after 2 weeks. From left to right, B_{10}, $B_{1\text{-}9}$.

For the wood carbon sample in olive oil testing, cases A_4 and A_6 showed the least amount of oil floating above the samples as can be seen from Figure 11(a). A_5 shows two groupings of oil and AC with the top layer of A_5 featuring smaller pellets of AC that have not clumped together to form a whole but floating together as individual pieces. The surface tension was likely affected during the production or agitation process.

During initial preparation, cotton-derived carbon was the most hydrophobic material and required extensive stirring to mix with the oil and even with the water. The cotton samples in Figure 11(b) exemplify the disparities in the effects of different acids. Case A_7 shows very weak adsorption capacity but features a bubble of oil in the middle of the tube and a lower one near the bottom. Microscopic testing could potentially reveal exactly which adsorbents are binding to a particular AC and how much more proficient one sample is versus another at adsorbing a specific compound.

Figure 11(c) shows the results of the used motor oil adsorption testing. Each sample contains about half of the original amount on the top surface of the test tube, so complete adsorption was not reached with 5 g of AC. Not all the components within the motor oil may be compatible with the AC, based on how much motor oil had not been adsorbed. However, from a glance, only the samples that were acidified with H_2SO_4 display similar patterns to the commercial AC. The patterns from case B_1 that span the entire length of the tube only cover the inner diameter of the tube, while the added water is stored behind it. In every case, a layer of AC and adsorbed oil had formed above the water. Future testing with different mediums, such as with a petri dish, may improve the accuracy of any observations. With commercial AC, there was an inadequate amount of AC in the adsorption environment, likely causing excess oil above the surface. 0.5 g of AC and 5 mL of adsorbents were tested against each other. As this sample represented the standard for which the other AC cases were tested, a conclusion can be reached that the AC to oil adsorption rate is less than 10:1, for the samples used in this study. Testing involving an appropriate amount of each AC with a base amount of used motor oil and olive oil would provide a more comprehensive indicator of the sample's effectiveness.

Utilizing the solidified, and exhausted AC that had formed underneath the fluid layer of motor oil, the test tubes were inverted and compared to better estimate how much AC had been adsorbed. Table 3 shows the volume of the remaining oil that was amassed on the top after 2 weeks.

Table 3. The remaining amount of motor oil after testing for two weeks.

Sample number	Material & treatment solution	Remaining oil (mL)
1	Commercial CAC	0.8
2	Paper, H_2SO_4	2.5
3	Paper, Lemon Juice	2.5
4	Paper, HCl	2.6
5	Wood, H_2SO_4	2.6
6	Wood, Lemon Juice	1.8
7	Wood, HCl	2.0
8	Cotton, H_2SO_4	2.3
9	Cotton, Lemon Juice	2.1
10	Cotton, HCl	2.3

The hardening in the motor oil cases was not present in the olive oil cases, which made for difficult oil extraction and measurement. Based on the volumes seen from the tubes and photos, the results of the olive oil testing showed that commercial AC was able to adsorb about 50% of the oil it was given. Comparatively, the paper samples were only capable of adsorbing half, presenting itself as the worst material in this study. Cotton had mixed results, with HCl being able to adsorb roughly 66% while lemon juice (LJ) adsorbed about 75%. Cotton H_2SO_4 only adsorbed about 50%. In contrast, the H_2SO_4, lemon juice, and HCl samples adsorbed 75%, 100%, and 50% of the oil respectively. Most of the cotton samples performed at the same level as or better than the commercial sample, and the wood samples all performed better.

For the motor oil samples, collecting results was largely successful due to the solidification that occurred from the AC samples adsorbing some components from the used motor oil. Although studies exist detailing the specific compositions of used motor oil, without more sophisticated equipment or analyses such as chromatography or spectroscopy, an understanding of what was adsorbed would be difficult to investigate [46]. Solely based on the amounts of remaining motor oil, the commercial AC performed the best, followed by wood, cotton, and paper. As a material, paper was consistently adsorbing about half of the original volume, while lemon juice appeared to be the activating reagent that contributed the most to increasing adsorption.

The adsorption capacity of AC was simultaneously observed during the evaporation tests. Results showed that the commercial sample had no difficulty adsorbing contaminants and seawater. In comparison, the lemon-juice-activated samples were murky and based on the clear distinction of a top and bottom layer, less consistent in activation. It may be more desirable to control the porosity of AC to optimize capturing specific components of an adsorbent while still maintaining a solar interface for evaporation.

To further extend our discussion, the rest of this section is dedicated to highlighting the feasibility of a reverse osmosis system that seeks to employ AC in its processes. One crucial part of demonstrating its viability is through the conducting of a meticulous cost-benefit analysis, which will include the costs of implementing AC, acquiring and processing AC, maintaining it, and disposing of it. Simultaneously, the environmental costs and potential benefits will also be discussed to provide an all-encompassing view of the situation.

Sorting is the first step in the waste-to-energy process, and it comes with several concerns, namely contamination, handling, and shipping. Cardboard refuse often yields traces of non-recyclable plastics, and often, clothing can be difficult to sort when the material is a blend of fabrics. From the carbonization process done in this experiment, it was also observed that different materials will carbonize at different rates, while exposed to the same heat source. Initial batches were observed for how long each sample took to carbonize, and it was discovered that paper, cardboard, cotton, and wood were the order for which samples would first completely carbonize.

The amount of carbon material converted, and fuel used for two batches were recorded. Nearly four times the weight of the initial materials is required for the completion of carbonization. The methods used initially are far from efficient and further experimentation with the temperature, heating duration, and pretreatment would be worthwhile subjects for improving yield and efficiency.

Additionally, it is important to consider the life cycle of the AC products used within the desalination plant. AC disposal or regeneration, maintaining a steady supply chain, and operation and maintenance costs are some of the important factors to evaluate. Disposal presents a unique challenge given that some of the adsorbents may present environmental hazards. Regeneration may be a more sustainable practice, but also comes with its own technological and financial costs. Foreseeably, the supply of recycled materials may be in surplus, but transportation costs as well as continued supply are also challenges. Production costs also carry with them the question of environmental offsets. A cost-benefit analysis would reveal the potential environmental tradeoffs for processing and activating carbon compared to a system that does not use it. Testing of the seawater input and the properties of the AC samples would allow for the most effective use and production.

It is estimated that to replace one ton of paper, 17 trees must be replanted [47]. Due to the relatively slow growth of trees compared to paper use, it may be in the best interests of sustainability to encourage paper recycling, based on the results of this study. To reconsider already scaled processes and pursue a new route in AC evaporation, a significantly high-performing AC made from paper or cardboard would have to be presented. If a large supply of recycled materials were locally available, cutting transportation costs would also make this proposition more appealing. In addition, if the environmental costs of manufacturing and employing AC as solar evaporators outweigh those of more sophisticated evaporators, it would also improve the outlook of this product. Current evaporators utilize more sophisticated structures and boast high evaporation rates of nearly 10 kg/m^2/h [48]. Comparatively, the AC used in this setting had an evaporation rate of roughly 1.39 kg/(m^2·h) in a 2-inch glass beaker requiring 72 hours of winter sunlight. The fastest sample at 49.45 hours has a calculated average evaporation rate of close to 1.93 kg/(m^2·h). The methods, results, and yield in this experiment point to carbonization as a high-cost process. Improved ovens, more sustainable heat sources, and heating containers would improve the quantity and quality of any charcoal used for fuel.

The oil absorption efficiency was compared with the existing work. In this work the sample with the best absorption efficiency is the commercial activated carbon, which achieved an

absorption efficiency of 84%. The wood derived carbon achieved 64%. It is noted that the oil absorption efficiency is calculated by:

$$\varepsilon = \frac{W_0 - W}{W_0} \times 100\% \quad (3)$$

where W is the weight of oil left after absorption; W_o is the initial oil weight.

Table 4 lists the performances of some products in the literature. While typical specimens from this research were also presented. The products based on nanofiber and aerogels are extremely absorptive. Almost all the spilled oil was cleaned completely by them [49, 50]. However, for some ordinary petroleum spill-clean materials such as porous concrete [51] or modified concrete [52], and fine sands [53], the calculated oil absorption efficiencies are in the range from 6 to 12% indicating they are not so good for oil absorption as the recycled carbon as prepared in this work. The derived carbon from recycled materials showed the oil absorption efficiencies around 60% as can be seen from the last several rows in Table 4. The commercial activated carbon has the oil absorption efficiency of 84% as tested by the same method in this study.

Table 4. Comparison of the oil absorption efficiency.

Material	Oil absorption efficiency	literature
Carbon foam	~100%	[49]
Cellulose nanofiber	~100%	[50]
Oil absorbent concrete[1]	10%	[51]
Hydrophobic modified concrete[1]	7%	[52]
Fine Sand	6~12%	[53]
Wood, Lemon Juice	64%	This work
Wood, HCl	60%	This work
Commercial activated carbon	84%	This work
Cotton, Lemon Juice	58%	This work
Cotton, HCl	54%	This work

[1] The density of concrete takes about 2.4 g/cm^3 which is used for the calculation here.

4. CONCLUSION

Activated charcoal (AC) is a cost-effective and easily implemented option for adsorption, evaporation, and desalination. Nonactivated carbon performed best in evaporation tests due to its ability to maintain a solar interface, while activated carbon, particularly wood-derived AC, excelled in salt adsorption. UV light can purify AC, allowing for potential desorption and collection of contaminants, and its high affinity for organic contaminants presents an

opportunity for microorganisms to break down and clean it. Quantitative thermal analysis revealed significant weight loss in wood between 285-350°C, with an exothermic peak at 345°C, and an ash content of about 3.5% when burned in air. Wood-derived carbon was about 30% more efficient in solar water desalination and sewage purification compared to commercial activated carbon. For oil absorption, lemon juice-treated carbon outperformed others by 40%, except for commercial activated carbon, which was 1.5 times more effective due to its high porosity. While this study shows promising preliminary results, scale-up applications must consider factors like demand, supply chain logistics, and material availability. Further research is necessary to explore different methods and types of AC for desalination. Despite some uncertainties, AC offers advantages over engineered materials due to its cost-effectiveness and accessibility, but thorough testing and research are essential to optimize its use in desalination, considering factors like carbonization time and the ideal AC-to-adsorbent ratios.

CONSENT FROM PATIENT

Not applicable.

ETHICAL APPROVAL FROM IRB

Not applicable.

REFERENCES

1. Nurjanah, I.; Chang, T. T.; You, S. J.; Huang, C. Y.; Sean, W. Y. Reverse osmosis integrated with renewable energy as sustainable technology: A review. *Desalination* **2024**, *581*, 117590; https://doi.org/10.1016/j.desal.2024.117590.

2. Kapepula, V. L.; Luis, P. Removal of heavy metals from wastewater using reverse osmosis. *Frontiers in Chemical Engineering* **2024**, *6*, 1334816; https://doi.org/10.3389/fceng.2024.1334816.

3. Okiel, K.; El-Sayed, M.; El-Kady, M.Y. Treatment of oil-water emulsions by adsorption onto activated carbon, bentonite, and deposited carbon. *Egyptian J. Petroleum* **2011**, *20* (2), 9-15; https://doi.org/10.1016/j.ejpe.2011.06.002.

4. Ganjoo, R.; Sharma, S.; Kumar, A.; Daouda, M.M.A. Chapter 1: Activated carbon: Fundamentals, classification, and properties, in *Activated Carbon Progress and Applications*, ed. Verma, C.; Quraishi, M.A. Hardback ISBN: 978-1-83916-780-5, PDF ISBN: 978-1-83916-986-1, EPUB ISBN: 978-1-83916-987-8, Roy. Soc. Chem. **2023**, pp. 1-22; https://doi.org/10.1039/BK9781839169861-00001.

5. Lu, Y.; Dai, T.Y.; Fan, D.Q.; Min, H.H.; Ding, S.; Yang, X.F. Turning trash into treasure: Pencil waste-derived materials for solar-powered water evaporation. Energy Technology 2020, 8 (10), 2000567; https://doi.org/10.1002/ente.202000567.

6. Wu, L.; Dong, Z.C.; Cai, Z.R.; Ganapathy, T.; Fang, N.X.; Li, C.X.; Yu, C.L.; Zhang, Y.; Song, Y.L. Highly efficient three-dimensional solar evaporator for high salinity desalination by localized crystallization. *Nature Comm.* **2020**, *11*, 521; https://doi.org/10.1038/s41467-020-14366-1.

7. Yang, M.; Bao, H.; Hu, X.M.; Sun, S.P.; Li, M.L.; Yan, Y.R.; Hou, W.J.; Cao, W.R.; Liu, H.; Wang, S.P.; Zhong, H.Z. Machine Learning Correlating Photovoltaics and

Electroluminescence of Quantum Dot Light-Emitting Diodes. *ACS Photonics* **2024**, *11* (5), 2131-2137; https://doi.org/10.1021/acsphotonics.4c00413.

8. Parikh, P.; Wang, R.; Meng, J. The potential and challenges of off-grid solar photovoltaics in resource-challenged settings: the case of sub-Saharan Africa. *Nature Reviews Materials* **2024**, *9* (3), 151-153; https://doi.org/10.1038/s41578-024-00660-7.

9. Hameiri, Z. Photovoltaics literature survey (No. 190). *Progress in Photovoltaics* **2024**, *32* (4), 276-279; https://doi.org/10.1002/pip.3795.

10. Hameiri, Z. Photovoltaics literature survey (No. 191). *Progress in Photovoltaics* **2024**, *32* (6), 417-422; https://doi.org/10.1002/pip.3809.

11. Lamberti, F.; Gatti, T. Crystal nano-engineering: A new era for perovskite photovoltaics. *Energychem* **2024**, *6* (2), 100118; https://doi.org/10.1016/j.enchem.2024.100118.

12. Zhou, Z.S.; Yuan, Z.Y.; Yin, Z.P.; Xue, Q.F.; Li, N.; Huang, F. Progress of semitransparent emerging photovoltaics for building integrated applications. *Green Energy & Environment* **2024**, *9*(6), 992-1015; https://doi.org/10.1016/j.gee.2023.05.006.

13. Li, C.; Sun, H.X.; Wang, M.; Gan, S.; Dou, D.; Li, L. High-performance pulse light stable perovskite indoor photovoltaics. *Science Bulletin* **2024**, *69* (3), 334-344; https://doi.org/10.1016/j.scib.2023.12.022.

14. Alnakeeb, M.A.; Hassan, M.A.; Teamah, M.A. Thermal performance analysis of corrugated plate solar air heater integrated with vortex generator. *Alexandria Engineering Journal* **2024**, *97*, 241-255; https://doi.org/10.1016/j.aej.2024.04.019.

15. Flores-Hernández, D.A.; Luviano-Juárez, A. Experimental platform for performance evaluation of thermoelectric generators. *IEEE Access* **2024**, *12*, 65471-65481; https://doi.org/10.1109/ACCESS.2024.3397922.

16. Kashyap, R.K.; Pillai, P.P. Plasmonic nanoparticles boost solar-to-electricity generation at ambient conditions. Nano Letters 2024, 24 (18) 5585-5592; https://doi.org/10.1021/acs.nanolett.4c00925.

17. Zhang, Y.W.; Liu, H.Z.; Zhou, X.F.; Hu, Z.Y.; Wang, H.; Kuang, M.; Li, J.M.; Zhang, H.C. A novel photo-thermal-electric hybrid system comprising evacuated U-tube solar collector and inhomogeneous thermoelectric generator toward efficient and stable operation. *Energy* **2024**, *292*, 130616; https://doi.org/10.1016/j.energy.2024.130616.

18. Hu, J.J.; Zhang, Y.R.; Xie, S.X.; Xiao, Y. Thermo-hydraulic performance of solar air heater with built-in one-eighth sphere vortex generators. *Applied Thermal Engineering* **2024**, *245*, 122837; https://doi.org/10.1016/j.applthermaleng.2024.122837.

19. Sabet, G.S.; Sari, A.; Fakhari, A.; Afsarimanesh, N.; Organ, D.; Hoseini, S.M. An experimental and numerical thermal flow analysis in a solar air collector with different Delta wing height ratios. *Frontiers in Heat and Mass Transfer* **2024**, *22*, 491-509; https://doi.org/10.32604/fhmt.2024.048290.

20. Xuan, Z.W.; Ge, M.H.; Zhao, C.Y.; Li, Y.Z.; Wang, S.X.; Zhao, Y.L. Effect of nonuniform solar radiation on the performance of solar thermoelectric generators. *Energy* **2024**, *290*, 130249; https://doi.org/10.1016/j.energy.2024.130249.

21. Zhao, P.Y.; Wu, C.C.; Li, Y.M. Design and application of solar sailing: A review on key technologies. *Chin. J. Aeronautics* **2023**, *36* (5), 125-144; https://doi.org/10.1016/j.cja.2022.11.002.

22. Quan, R.H.; Xu, M.W.; Yao, Y.J. Three-dimensional particle tracing analysis of a rotational magnetic sail, *AIAA Journal* **2024** *62* (6), 2214-2221; https://doi.org/10.2514/1.J063337.

23. Boni, L.; Bassetto, M.; Quarta, A.A. Characterization of a solar sail membrane for Abaqus-based simulations. *Aerospace* **2024**, *11* (2), 151; https://doi.org/10.3390/aerospace11020151.

24. Mengali, G.; Quarta, A.A. Optimal trajectories of diffractive sail to highly inclined heliocentric orbits. *Applied Sciences-Basel* **2024**, *14* (7), 2922; https://doi.org/10.3390/app14072922.

25. Malhas, R.N.; Amadi, K.W. Oil removal from polluted seawater using carbon avocado peel as bio-absorbent. *European J. Eng. Technol. Res.* **2023**, *8*(2), 26–32; https://doi.org/10.24018/ejeng.2023.8.2.3004.

26. Chen, W.; Xiao, S.; Liu, Y.; Hu, X.; Xie, Y.; Liu, Y.; Ma, Y.; Luo, L.; Jiang, X. MXene-decorated bio-based porous carbon composite phase change material for superior solar-thermal energy storage and thermal management of electronic components. *J. Mater. Res. Technol.* **2023**, *27*, 1857-1873; https://doi.org/10.1016/j.jmrt.2023.10.081.

27. Yang, L.Y.; Qiu, J.; Wang, Y.; Guo, S.; Feng, Y.; Dong, D.; Yao, J.F. Molten salt synthesis of hierarchical porous carbon from wood sawdust for supercapacitors. *J. Electroanalytical Chem.* **2020**, *856*, 113673; https://doi.org/10.1016/j.jelechem.2019.113673.

28. Ji, T.; Chen, L.; Mu, L.W.; Yuan, R.X.; Knoblauch, M.; Bao, F.S.; Shi, Y.J.; Wang, H.Y.; Zhu, J.H. Green processing of plant biomass into mesoporous carbon as catalyst support. *Chem. Eng. J.* **2016**, *295*, 301-308; https://doi.org/10.1016/j.cej.2016.03.033.

29. Tsyganova, S.I.; Korolkova, I.V.; Bondarenko, G.V.; Kargin, V.F. Formation of the pore structure of modified wood by treatment with heat and water. *Russian J. Appl. Chem*. **2011**, *84* (11), 1997-2001; https://doi.org/10.1134/S1070427211110280.

30. Chen, C.; Kuang, Y.; Zhu, S.; Burgert, I.; Keplinger, T.; Gong, A.; Li, T.; Berglund, L.; Eichhorn, S.J.; Hu, L.B. Structure–property–function relationships of natural and engineered wood. *Nat. Rev. Mater.* **2020**, *5*, 642–666; https://doi.org/10.1038/s41578-020-0195-z.

31. Luo, M.; Yang, K.; Zhang, D.T.; Liu, C.Z.; Yang, P.; Chen, W.M.; Zhou, X.Y. Lignocellulose-based free-standing hybrid electrode with natural vessels-retained, hierarchically pores-constructed and active materials-loaded for high-performance

hybrid oxide supercapacitor. *Int. J. Bio. Macromolecules* **2021**, *187*, 903-910; https://doi.org/10.1016/j.ijbiomac.2021.07.178.

32. Hao, Y.X.; Qian, M.; Xu, J.J.; Bi, H.; Huang, F.Q. Porous cotton-derived carbon: Synthesis, microstructure and supercapacitive performance. *J. Inorganic Mater.* **2018**, *33* (1), 93; https://doi.org/10.15541/jim20170164.

33. Thach, N.K.; Krechetov, I.S.; Berestov, V.V.; Kan, O.; Maslochenko, Maslochenko, I.A.; Lepkova, T.L.; Stakhanova, S. The role and effect of CO_2 flow rate on the structure formation of ultrahigh porous activated carbon from H_3PO_4-impregnated waste cotton used as supercapacitor electrode material. *Nanosystems-Physics Chemistry Mathematics* **2023**, *14* (4), 489-497; https://doi.org/10.17586/2220-8054-2023-14-4-489-497.

34. Li, Z.Z.; Yu, L.J.; Ma, H.D.; Chen, J.L.; Meng, J.G.; Wang, Y.Z.; Liu, Y.M.; Song, Q.W.; Dong, Z.J.; Miao, M.H.; Li, B.; Zhi, C. An efficient interfacial solar evaporator featuring a hierarchical porous structure entirely derived from waste cotton. *Sci. Total Environ.* **2023**, *903*, 166212; https://doi.org/10.1016/j.scitotenv.2023.166212.

35. Shi, G.G.; Wu, M.M.; Zhong, Q.; Mu, P.; Li, J. Superhydrophobic waste cardboard aerogels as effective and reusable oil absorbents. *Langmuir* **2021**, 37 (25), 7843-7850; https://doi.org/10.1021/acs.langmuir.1c01216.

36. Shimada, M.; Hamabe, H.; Iida, T.; Kawarada, K.; Okayama, T. The properties of activated carbon made from waste newsprint paper. J. Porous Mater. **1999**, *6* (3), 191-196; https://doi.org/10.1023/A:1009671711925.

37. Matsushita, K.; Shimada, M.; Okayama, T. Adsorption properties of bisphenol A on activated carbon prepared from wastepaper. *Sen-I Gakkaishi* **2009**, *65* (11), 287-291.

38. Crespo-Lopez, L.; Coletti, C.; Morales-Ruano, S.; Cultrone, G. Use of recycled carbon fiber as an additive in the manufacture of porous bricks more durable against salt crystallization. *Ceramics Int.* **2024**, *50* (6), 9682-9696; https://doi.org/10.1016/j.ceramint.2023.12.287.

39. Zhao, Z.C.; Lin, L.; Zhang, J.; Xu, B.; Ma, Y.B.; Li, J. A green approach to enhance the adsorption capacity: Synthesis of bamboo-based adsorbent by biological pretreatment. *Ind. Crop. Products* **2024**, *213*, 118388; https://doi.org/10.1016/j.indcrop.2024.118388.

40. Murugesan, M.; Nagavenkatesh, K.R.; Devendran, P.; Nallamuthu, N.; Kumar, M.K.; Ramesh, K. Preparation and electrochemical investigation of NiO hollow sphere from bio waste (sugarcane bagasse) extract for energy storage applications. *J. Inorg. Organometallic Poly. Mater.* **2024**, early access at https://doi.org/10.1007/s10904-024-03044-0.

41. Gautam, M.K.; Mondal, T.; Nath, R.; Mahajon, B.; Chincholikar, M.; Bose, A.; Das, D.; Das, R.; Mondal, S. Harnessing activated hydrochars: A novel approach for pharmaceutical contaminant removal. *C-Journal of Carbon Research* **2024**, 10 (1), 8; https://doi.org/10.3390/c10010008.

42. Lee, W.J.; Kwon, S.H.; Role of acid treatment of the carbon support in the growth of atomic-layer-deposited Pt nanoparticles for PEMFC fabrication. *Particles & Particle Syst. Charact.* **2023**, *40* (2), 2200158; https://doi.org/10.1002/ppsc.202200158.

43. Zhu, L.; Gao, M.; Peh, C. K. N.; Ho, G. W. Recent progress in solar-driven interfacial water evaporation: Advanced designs and applications. *Nano Energy* **2019**, *57*, 507-518; https://doi.org/10.1016/j.nanoen.2018.12.046.

44. Santos, D.H.S.; Duarte, J. L.S.; Tonholo, J.; Meili, L.; Zanta, C.L.P.S. Saturated activated carbon regeneration by UV-light, H_2O_2 and Fenton reaction. *Separation and Purification Technology* **2020**, *250*, 117112; https://doi.org/10.1016/j.seppur.2020.117112.

45. Januszewicz, K.; Kazimierski, P.; Klein, M.; Kardas, D.; Łuczak, J. Activated carbon produced by pyrolysis of waste wood and straw for potential wastewater adsorption. *Materials* **2020**, 13, 2047; https://doi.org/10.3390/ma13092047.

46. Syrmanova, K.K.; Kovaleva, A.Y.; Kaldebekova, Z.B.; Botabayev, N.Y.; Botashev, Y.T.; Beloborodov, B.Y. Chemistry and recycling technology of used motor oil. *Oriental Journal of Chemistry*. **2017**, *33* (6), 3195-3199; http://dx.doi.org/10.13005/ojc/330665.

47. Moosavi, M., Ghorbannezhad, P, Azizi, M., Hosseinabadi, H. M., Evaluation of life cycle assessment in a paper manufacture by analytical hierarchy process. *Int. J. Sustainable Eng.* **2021**, *14* (107), 1-11; http://dx.doi.org/10.1080/19397038.2021.1982065.

48. Chen, Y.; Wang, Y.; Xu, J.; Raihan, M.R.I.; Guo, B.; Yang, G.; Li, M.; Bao, H.; Xu, H. A 3D opened hollow photothermal evaporator for highly efficient solar steam generation. *RRL Solar* **2022**, *6* (7), 2200202; https://doi.org/10.1002/solr.202200202.

49. Qu, J.Y.; Han, Q.; Gao, F.; Qiu, J.S. Carbon foams produced from lignin-phenol-formaldehyde resin for oil/water separation. *New Carbon Materials* **2024**, *32* (1), 86-91; https://doi.org/10.1016/S1872-5805(17)601094.

50. Miao, Y.; Liang, Y.P.; Wang, E.F.; Dai, C.P.; Ren, C.Y.; Cao, Y.Z.; Zou, L.H.; Zhang, W.B.; Huang, J.D. Magnetic superhydrophobic cellulose nanofibril based aerogel with rope-ladder like structure incorporating both superelasticity and excellent oil absorption. *Journal of Environmental Management* **2024**, *358*, 120909; https://doi.org/10.1016/j.jenvman.2024.120909.

51. Wang, D.L.; Yang, Z.Y.; Zheng, H.J.; Li, K.; Pan, H.M.; Li, T. Research on the mechanism of strength improvement in acid-base-activated low carbon oil absorbent concrete. *Sustainability*, **2024**, *16* (9), 3661; https://doi.org/10.3390/su16093661.

52. Wang, D.L.; Wu, X.M.; Yuan, L.L.; Wu, D.H.; Zhao, Q.X.; Pan, H.M.; Qi, W.Y. Oil absorption and plant symbiosis capacity of hydrophobic modified concrete: Preparation and performance analysis. *Construction and Building Materials* **2024**, *413*, 134897; https://doi.org/10.1016/j.conbuildmat.2024.134897.

53. Abousnina, R.M.; Manalo, A.; Shiau, J.; Lokuge, W. Effects of light crude oil contamination on the physical and mechanical properties of fine sand. *Soil and*

Sediment Contamination: An International Journal **2015**, *24* (8), 833-845; https://doi.org/10.1080/15320383.2015.1058338.